A Quasiclassical Trajectory Study of Collisional Energy Transfer and Dissociation in He + H_2(v,j) Using a New Potential Energy Surface†

M. E. Mandy* and G. J. McNamara

Program in Chemistry, University of Northern British Columbia, Prince George, British Columbia, V2N 4Z9 Canada

Received: June 2, 2005; In Final Form: August 12, 2005

Quasiclassical trajectories for He + H_2 were carried out using the recent ab initio potential of Boothroyd, Martin, and Peterson (*J. Chem. Phys.* **2003**, *119*, 3187) and results for the 348 (v, j) states of H_2 are compared to those of earlier calculations that used the potential of Wilson, Kapral, and Burns (*Chem. Phys. Lett.* **1974**, *24*, 4884). Examined are the cross sections for energy transfer and dissociation, the extent of threshold elevation, and the interconversion of vibrational and rotational energy. Implications for modeling the interstellar medium are discussed.

1. Introduction

Recently Boothroyd, Martin, and Peterson (BMP) published a new analytic potential energy surface (PES) determined by a fit to over 20 000 ab initio points they had calculated for He + H_2.[1] This new surface represents a significant improvement on earlier potential energy surfaces for He + H_2[2−16] and provides a PES comparable in accuracy to those available for 2^{17-21} and He + H_2.[22−25]

Most of the earlier PESs for He + H_2 were restricted to particular regions of conformation space where the H−H distances are short. These potentials are suitable for calculations such as the determination of transport and relaxation properties of H_2 in He (cf. McCourt et al.[26] and references therein) and the characterization of van der Waals complexes (cf. Kalinin et al.[27] and Gianturco et al.[28] and references therein). Some of these potentials were also useful for quantum calculations (cf. Lee et al.[29] and references therein).

The PES of Wilson, Kapral, and Burns[9] (WKB) was an exception in that it attempted to cover the entire region of conformation space. Regions where the H−H separations are large are important for dissociation and excitation to high levels of vibration or rotation. Extensive quasiclassical calculations have been carried out on the WKB PES as modified by Dove and Raynor.[12] These calculations were motivated by the necessity for a complete set of state-to-state rate coefficients that could be used in master equation calculations[30] in temperature and density regimes typical of the interstellar medium.

Molecular hydrogen is the dominant molecular species in the interstellar medium and is found in giant molecular clouds. Shocks in these clouds are associated with star formation, and an understanding of how shock heated hydrogen gas cools in the wake of a shock is desirable.[31] Since after atomic H, He is the next most abundant atomic species, collisions of He with H_2 are expected to play a role. Densities in the interstellar medium can be quite low and radiative processes (i.e., quadrupole emission in the infrared) can compete with the collisional processes. In addition to dissociative cooling, the removal of energy by emission after collisional excitation can contribute to the cooling. In their master equation calculations, Dove and co-workers[30] explored the density and temperature dependence of cooling for H_2 infinitely dilute in He. Their results were limited by the accuracy of the WKB results.

2. Potential Energy Surfaces

In Figure 1 are shown some representative cuts of both the BMP and WKB PESs, along with the corresponding difference plots. The collinear cuts correspond to the three atoms in a straight line with He at the terminal position, while the perpendicular cuts correspond to the approach of the He atom along a line bisecting the axis between the two H atoms. Figure 1a shows the collinear cut of the BMP PES. A small value of R_2 with a large value of R_1 corresponds to a bound H_2 molecule far from the He, and the R_2 dependence extrapolates to the potential of an isolated H_2 molecule as R_1 increases. Small values of R_1 and R_2 correspond to He interacting closely with H_2. For such conformations, the interaction potential is steeply repulsive. The collinear cut of the WKB PES (Figure 1b) also shows a repulsive wall, but this wall has a "hole" in that for certain values of R_1 and R_2, the potential becomes steeply negative and unphysical. This mathematical artifact arises because there were no ab initio points available to Wilson et al.[9] in this region to constrain the fitting function. Conformations in this region would be encountered only at high collision energies, but this region has implications for dissociation or excitation to the higher energy (v, j) states. Figure 1c illustrates the differences (BMP PES − WKB PES) in the two potentials. Immediately evident are the differences in the shape of the end of the valley and of the repulsive wall. Both of these regions are expected to have a significant effect on the outcomes of collisions of He + H_2. The shape of the end of the entrance valley influences energy transfer behavior, while the shape of the repulsive wall determines whether a collision leads to dissociation or to excitation of the molecule.

The perpendicular conformations are addressed in Figure 1d−f. The earlier work of Mandy[32] showed that collisions involving perpendicular conformations were more likely to lead to dissociative outcomes than other angles of approach, especially near the threshold for dissociation. For this conformation, the repulsive wall of the WKB PES is significant for larger values of R_1 than is the case of the BMP PES. The difference plot

† Part of the special issue "Donald G. Truhlar Festschrift".

10.1021/jp0529319 CCC: $33.50
Published on Web 09/30/2005

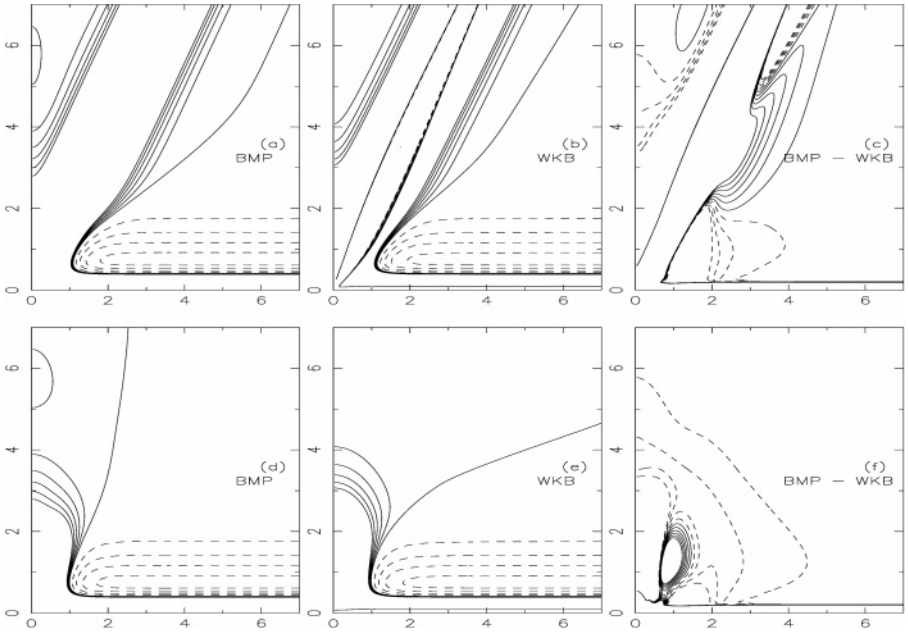

Figure 1. Comparison of the potential energy surface of Boothroyd et al. with that of Wilson et al.: (a−c) collinear cuts of the BMP surface, the WKB surface, and the (BMP−WKB) difference surface, respectively; (d−f) corresponding plots for the perpendicular cut of the potential energy surfaces. The horizontal axis is R_1, the separation of the He atom from the center of mass of the 2 system, while the vertical axis is R_2, the distance between the two H atoms. Both R_1 and R_2 are in units of Å. In parts a, b, d, and e, the dashed contours are at 25 kcal mol^{-1} intervals below the limit of three atoms infinitely separated, while the solid contours corresponds to interval of 100 kcal mol^{-1} above the same limit. In the difference surface, parts c and f, the dashed contours are for negative differences at intervals of 1 kcal mol^{-1}, while the solid contours are for positive differences at the same interval of 1 kcal mol^{-1}.

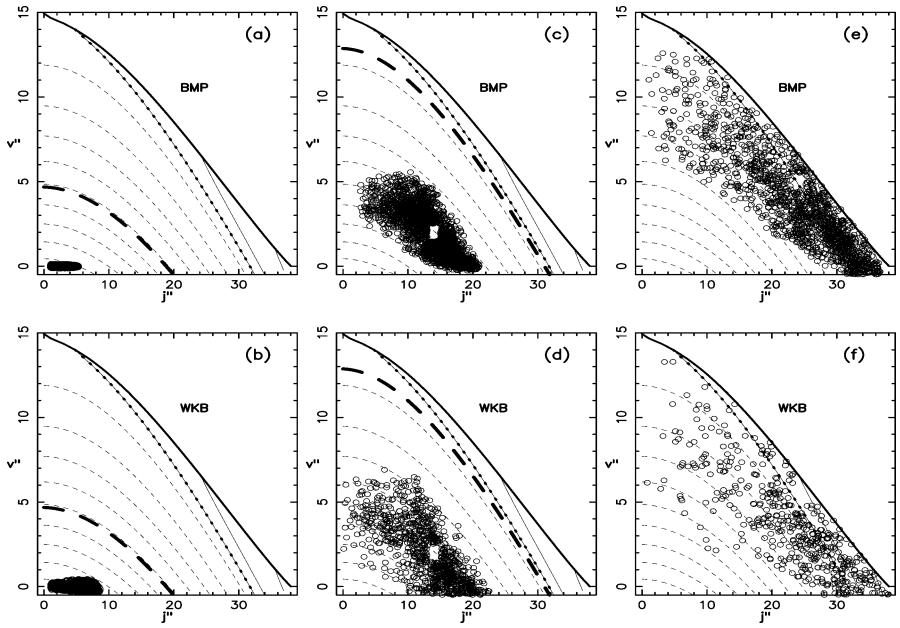

Figure 2. Comparison of the distributions of final continuously valued QCT "quantum numbers" for inelastic trajectory results in the lowest stratum of impact parameter (0.0−0.5 Å): (a) for He + H_2(0,0) on the BMP PES, (b) for He + H_2(0,0) on the WKB PES, (c) for He + H_2(2,14) on the BMP PES, (d) for He + H_2(2,14) on the WKB PES, (e) for He + H_2(5,24) on the BMP PES, and (f) for He + H_2(5,24) on the WKB PES. In all cases the translational energy is 50 kcal mol^{-1} and the total energy of the system is indicated by the heavy dashed line. Other contours are given at 12.5 kcal mol^{-1} intervals, on an energy scale relative to the potential energy minimum of H_2. The heavy solid line represents the dissociation limit while the beaded contour represents the rotationless dissociation limit.

(Figure 1f) shows the qualitative and quantitative differences between the two plots, particularly in the shape of the repulsive wall.

Processes at high total energy, such as collision-induced dissociation and energy transfer at high translational energy, have been explored using the WKB PES.[32−35] At the time, it was the only global PES available for He + H_2. However, these calculations were limited in their validity because of the unphysical hole in the repulsive wall. The integration of significant numbers of trajectories failed when this region of the potential was encountered.

For this reason, calculations on an improved potential were deemed necessary. In this paper we examine collisional energy transfer, collision-induced dissociation and elevation of thresholds for these processes using the BMP potential and compare our results with those obtained using the WKB PES.

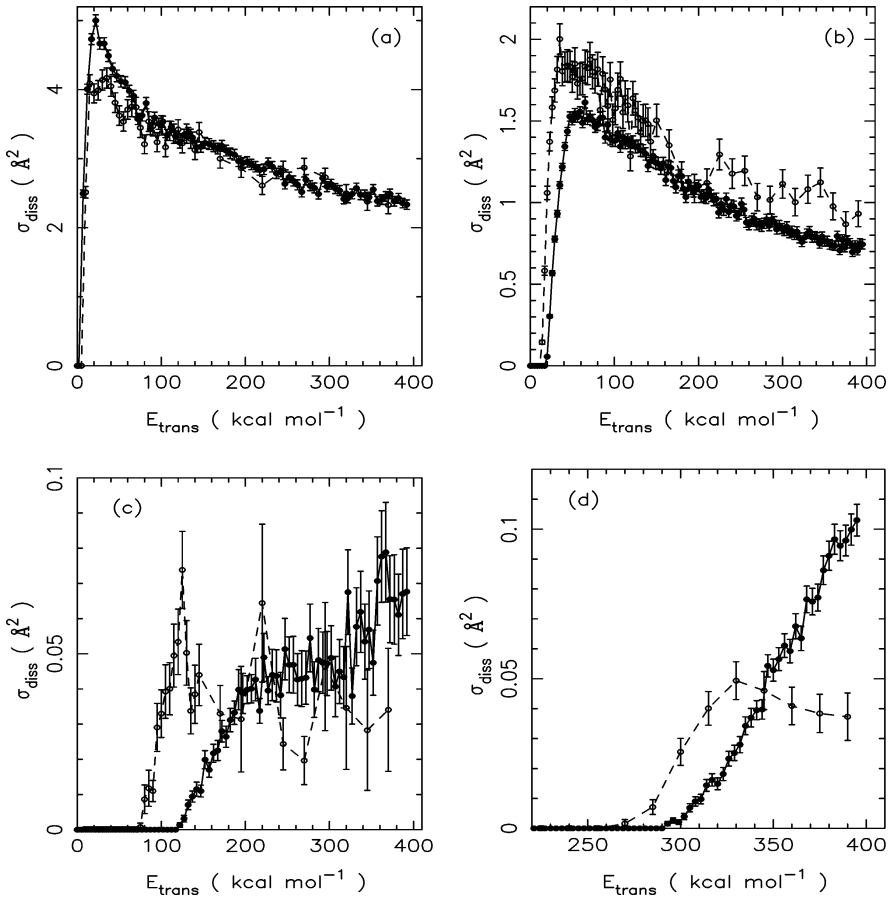

Figure 3. Comparison of state-to-state cross sections determined from quasiclassical trajectories using the BMP PES (solid circles) and the WKB PES (open circles) for the following transitions: (a) He + H_2(0,0) → He + H_2(0,2); (b) He + H_2(0,0) → He + H_2(0,4); (c) He + H_2(0,0) → He + H_2(1,0); (d) He + H_2(0,0) → He + H + H.

3. Method

Cross sections for state-to-state energy transfer and dissociation were calculated by the quasiclassical trajectory (QCT) method using the potential energy surfaces of Boothroyd et al.[1] and Wilson et al.[9] All trajectories were initiated with internal energy corresponding precisely to one of the 348 (v, j) states of the H_2 molecule. The initial relative translational energy was also specified. Stratified sampling was used for the impact parameter and all other parameters were Monte Carlo selected as described in Dove and Raynor.[12] In the QCT method, the collision is treated classically throughout and the equations of motion were integrated using the Adams' predictor-corrector method with a fixed step size of 5×10^{-20} s.[36] The desired accuracy of integration (energy conservation within 0.005 kcal mol^{-1}) was achieved using 7 as the order of the integrator.

The outcome of each nondissociative trajectory was analyzed for vibrational and rotational quasiclassical quantum numbers from a continuous (v, j) range. A minimum of 3000 trajectories per impact parameter stratum for each energy was calculated on the BMP PES. To ensure convergence of the cross section, successive impact parameter strata were considered until all collisions were observed to be elastic. For each (v, j) state, trajectories were run at translational energy intervals of 1 kcal mol^{-1} from 399 kcal mol^{-1} down to either 1 kcal mol^{-1} or to a translational energy at which all trajectories were observed to be elastic. The calculations using the WKB PES had been carried out when computational facilities were more constrained. These runs on the WKB PES had used 1000 trajectories per impact parameter strata. Intervals of 5 kcal mol^{-1} were used between energies of 400 and 20 kcal mol^{-1} above the energetic threshold to dissociation followed by intervals of 1 kcal mol^{-1} below that. Further details of the method of calculation are described elsewhere.[12,33,34,37,38]

There is no exchange channel for the He−H_2 system, so only nonreactive or dissociative outcomes are possible. The nonreactive trajectories were binned as described by Dove, Raynor, and Teitelbaum[35] with the modifications of Mandy and Martin.[37]

Statistical errors on all cross sections were calculated. Since we were considering processes with probabilities P_i that could be of the order of $1/N_i$, we used[39]

$$\sigma \pm d\sigma = \sum_i P_i A_i \pm \sqrt{\sum_i A_i^2 \left[\frac{P_i(1-P_i)}{N_i} + \frac{1}{N_i^2} + \frac{1}{N_i^3}\right] \Big/ \left[\left(1+\frac{3}{N_i}\right)\left(1+\frac{2}{N_i}\right)^2\right]} \quad (1)$$

where N_i is the number of trajectories in the batch and A_i is the area of the impact parameter annulus associated with the ith impact parameter stratum. This permits us to estimate the errors on statistically null cross sections.

4. Results and Discussion

First, the overall energy transfer behavior is considered. Figure 2 shows the values of the final continuously valued QCT "quantum numbers" for three representative states at a translational energy of 50 kcal mol^{-1} on each of the potential energy

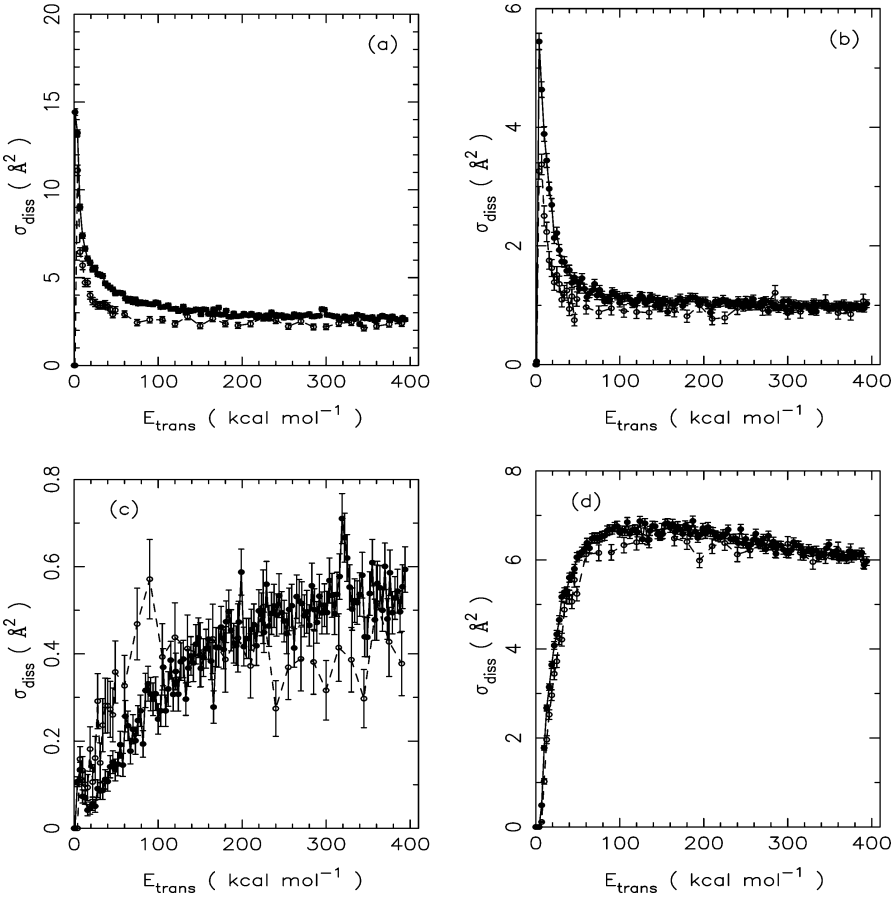

Figure 4. Comparison of state-to-state cross sections determined from quasiclassical trajectories using the BMP PES (solid circles) and the WKB PES (open circles) for the following transitions: (a) He + H_2(12,0) → He + H_2(12,2); (b) He + H_2(12,0) → He + H_2(12,4); (c) He + H_2(12,0) → He + H_2(13,0); (d) He + H_2(12,0) → He + H + H.

surfaces. Energy transfer from H_2(0,0) is dominated by rotational excitation and is much more limited for the BMP PES than it is for the WKB PES. Also considered is H_2(2,14), a state with approximately equal energy in vibration and rotation. For both potentials, the energy transfer is dominated by interconversion of vibrational and rotational energy with the observed pattern much more compact for the BMP PES than for the WKB PES. A number of other states at other translational energies were examined, leading to the conclusion that there is less energy transfer overall for the BMP PES than was observed for the WKB PES for initial states (v, j) of low to moderate internal energy.

The situation is similar for states closer to the dissociation limit. In Figure 2, parts e and f, are shown the results for energy transfer from H_2(5,24) for the BMP PES and WKB PES, respectively. As in the case of H_2(2,14), the internal energy is approximately equally divided between vibration and rotation and the energy transfer is dominated by interconversion of vibrational and rotational energy. The distribution arising from the WKB PES exhibits more deexcitation in both v and j than is observed for the BMP PES.

In Figure 3 are shown cross sections for selected transitions from H_2(0,0) plotted against translational energy. Figure 3a is for rotational excitation from H_2(0,0) to H_2(0,2). Both potential energy surfaces give rise to similar behavior of the cross section with respect to energy with those from the BMP PES peaking more sharply near threshold. Differences are more pronounced in Figure 3b which shows the cross sections for transitions from H_2(0,0) to H_2(0,4). Consistent with the dampening of energy transfer with the BMP PES observed in Figure 2, the BMP cross sections are consistently below the WKB cross sections and exhibit some elevation of the threshold for the transition. These effects are even more pronounced for the transition from H_2(0,0) to H_2(1,0) (Figure 3c). With this extent of threshold elevation evident, the corresponding rate coefficients will be much lower than those determined from the WKB PES, especially at low temperatures where the value of the rate coefficient will be dominated by the values of the cross sections near threshold.

The differences in the cross sections for collision-induced dissociation from H_2(0,0) shown in Figure 3d are very pronounced. The BMP PES gives rise to dissociation cross sections that have a larger elevation of threshold and continue to increase monotonically, while those from the WKB PES have a maximum and then decrease. The latter behavior is an artifact of the unphysical behavior of the WKB potential. As the translational energy is increased above that at which collision-induced dissociation is first observed, an increasing number of trajectories fail as they enter the unphysical "hole" on the WKB PES. At the highest energies considered, the number of failed trajectories is comparable to the number of dissociative trajectories, casting doubt upon the validity of the WKB dissociation cross sections at those energies.

The differences due to the PESs are not as pronounced for transitions from H_2(12,0). Again for rotational excitation by two quanta (Figure 4a), the cross sections peak sharply at threshold with those from the BMP PES only slightly larger than those from the WKB PES. For the transition from H_2(12,0) to H_2(12,4) shown in Figure 4b, the cross sections from the BMP PES are consistently above those from the WKB PES and exhibit no greater threshold elevation. This is the opposite of what

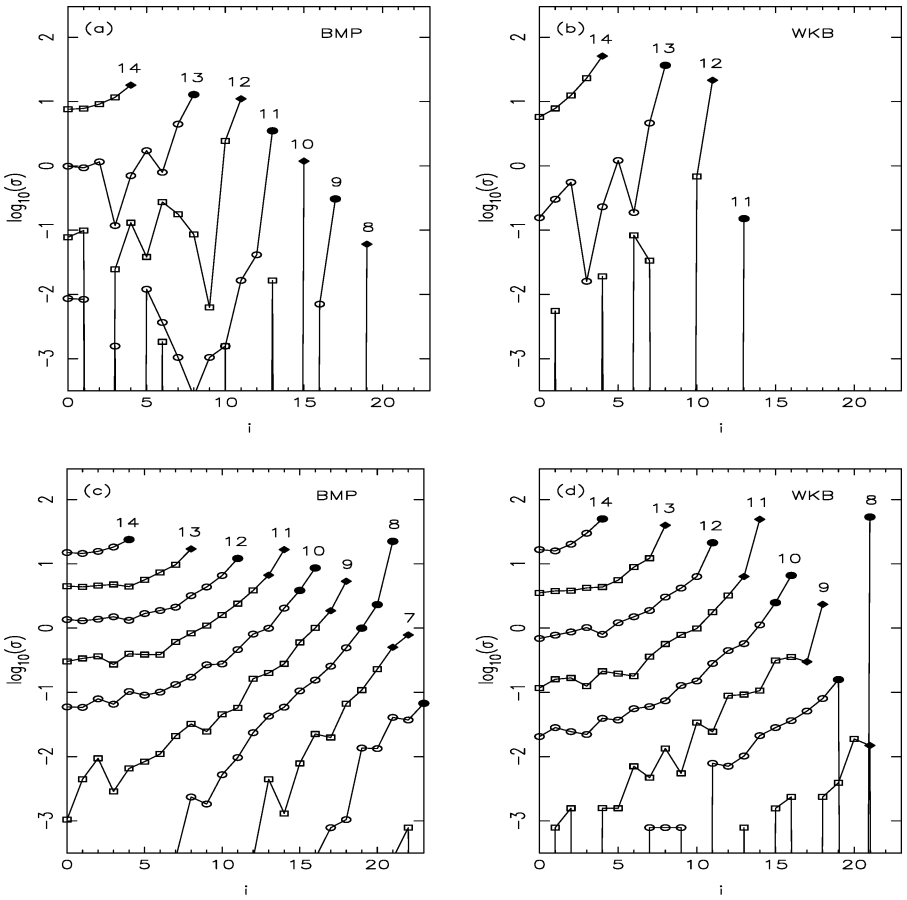

Figure 5. Base 10 logarithm of dissociation cross sections in Å^2 as a function of rotational quantum number. The states within each vibrational manifold are joined by a solid line labeled with the vibrational quantum number. The solid symbols are quasibound states, while the open symbols are for states with internal energy below the dissociation limit. $E_{tot} = 110$ kcal mol^{-1} for (a) BMP PES and (b) WKB PES; $E_{tot} = 114$ kcal mol^{-1} for (c) BMP PES and (d) WKB PES.

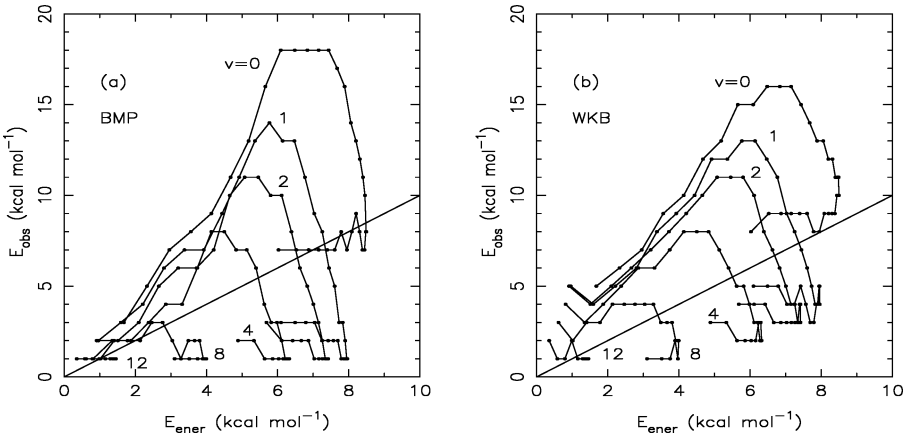

Figure 6. Observed dynamic threshold energy plotted against energetic threshold for He + H_2 (v, j) → He + H_2(v, j + 2) for rotational manifolds of selected vibrational states on (a) the BMP PES and (b) the WKB PES. The straight line indicates the energetic threshold. All energies are in kcal mol^{-1}.

happened for the transition from H_2(0,0) to H_2(0,4) (Figure 4b). No noticeable difference in threshold is observed for vibrational excitation from H_2(12,0) to H_2(13,0) (Figure 4c) or for dissociation (Figure 4d). Thus, it appears that differences due to the PES in elevation of the threshold depend on the initial state of the molecule.

This effect is explored further by examining dissociation cross sections at total energies slightly above 109.5 kcal mol^{-1}, the energetic requirement for dissociation. Figure 5 shows cross sections for a number of states at total energies of 110 kcal mol^{-1} and 114 kcal mol^{-1}. These cross sections are examined as a function of the rotational quantum number j for a series of rotational manifolds associated each with a particular vibrational state. All states considered are highly excited with internal energy in excess of half that required for dissociation. Increasing the internal energy as rotational energy has the general effect of increasing the dissociation cross sections while increasing the internal energy as vibration has an even more pronounced effect. Generally, the dissociation cross sections determined using the BMP PES are smaller than those of the WKB PES at

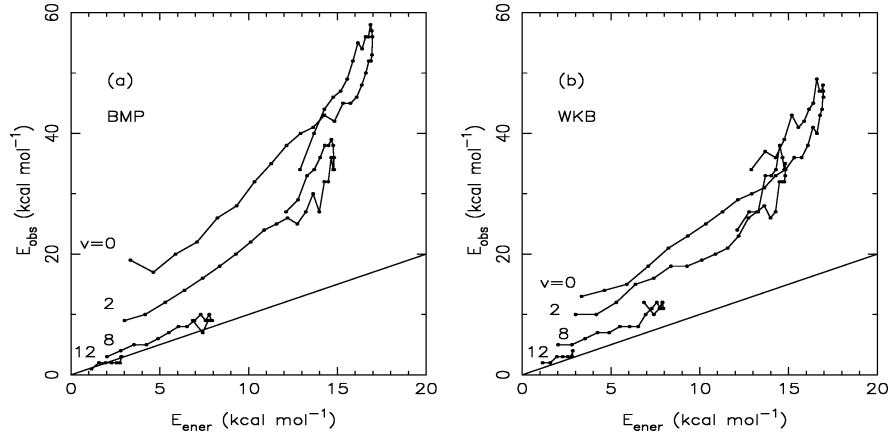

Figure 7. As in Figure 6, but for He + $H_2(v, j) \rightarrow$ He + $H_2(v, j + 4)$.

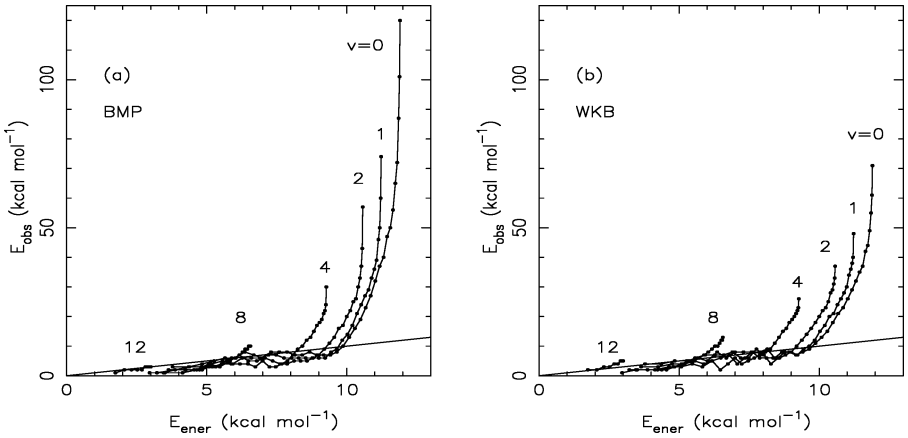

Figure 8. As in Figure 6, but for He + $H_2(v, j) \rightarrow$ He + $H_2(v + 1, j)$.

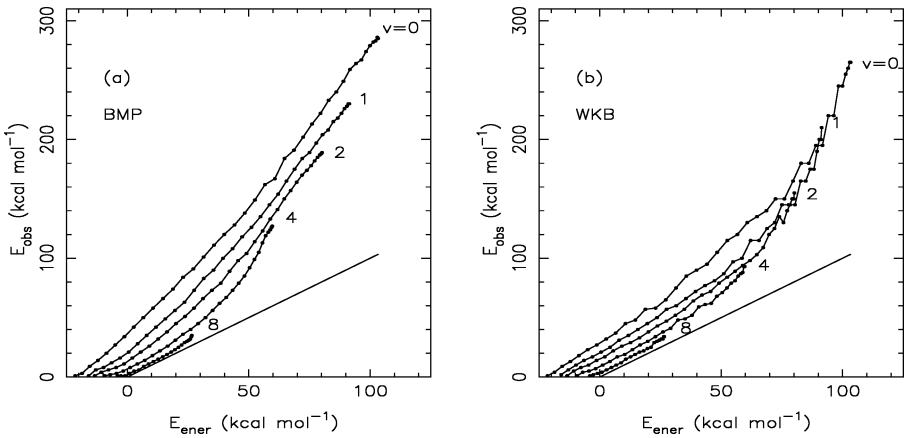

Figure 9. As in Figure 6, but for He + $H_2(v, j) \rightarrow$ He + H +H.

the total energy of 110 kcal mol^{-1}. At the slightly higher total energy of 114 kcal mol^{-1}, the cross sections from the BMP PES are smaller than the WKB for $v > 12$, but the situation is reversed for lower values of v. When compared to results on the WKB PES, this means that while greater dynamic elevation of the threshold to dissociation is the case for lower states on the BMP PES, this is not always the case for more excited states.

Now considered is the relative extent of threshold elevation on the two different PESs for various transitions. In Figure 6, the observed threshold is compared with the energetic threshold for rotational excitation by two quantum numbers, while the vibrational quantum number remains unchanged. Since H_2 is homonuclear, rotational transitions are restricted to changes of an even number of rotational quanta. Thus, $\Delta v = 0$, $\Delta j = 2$ is the smallest transition that can be made by H_2 in a low state. To be noted is that, due to effects of vibrational rotational coupling, the energy required for this transition does not increase monotonically with rotational quantum number for a particular value of v. For low values of j, the energetic requirement for the transition increases, then at high values of j, starts to decrease. (This accounts for the shapes of the rotational manifolds shown in Figure 6.) Also to be noted is that some of the observed thresholds are below the energetic thresholds. This is due to the fact that the binning of the trajectory results can assign a result to a state with a final rotational quantum number infinitesimally larger than $j + 1$. This "barely-in-the-box" effect is discussed extensively elsewhere[40] and is a consequence of the quasiclassical treatment. Inspection of these figures shows

that, for $v < 12$, the elevation of the observed threshold is much more pronounced for the BMP PES than for the WKB PES. This is consistent with the behavior illustrated in Figures 2−4.

Threshold elevation is also evident for transitions with $\Delta v = 0$, $\Delta j = 4$, with greater elevation observed for the BMP PES than for WKB PES for states with $v < 8$ as shown in Figure 7. As was noted for Figure 6, the energetic thresholds do not increase monotonically with j and a few observed thresholds are less than energetic.

In Figure 8 are shown the observed thresholds for transitions which increase v by one unit without changing j. Observed thresholds below the energetic thresholds are due to the "barely in-the-box" effect where final vibrational quantum numbers above $v + {}^1/_2$ are regarded as having undergone a vibrational transition. Again much more elevation of threshold is observed for the low initial v states on the BMP PES than for the WKB PES, while for higher initial v states, the situation in inverted.

The observed thresholds for collision-induced dissociation are considered in Figure 9. Negative energetic thresholds are associated with the quasibound states. The quasibound states have internal energies in excess of the dissociation limit, but are bound by the rotational barrier. Such states may tunnel through the barrier to dissociation. In many cases, elevation of the threshold for dissociation is observed. This is more pronounced for states of low internal energy than for states with higher internal energy. A greater elevation of threshold was observed for the BMP PES than for the WKB PES.

5. Future Directions

It is clear that cross sections for all processes considered in this paper that are calculated using the BMP PES can differ considerably both qualitatively and quantitatively from those determined using the WKB PES. Thus, a complete calculation of all the state-to-state and dissociation cross sections and rate coefficients has been undertaken using the BMP PES. It is quite likely that the master equation calculations of Dove et al.[30] will yield different results when repeated with rate coefficients determined from the BMP PES. To facilitate these master equation calculations, the rate coefficients will be made available parametrized as a function of temperature.[41] A detailed comparison of classical and quantum calculations is also planned.

Acknowledgment. This work was supported by a grant from the Natural Sciences and Engineering Research Council of Canada. The calculations were carried out using the high performance computing facility jointly supported by the Canadian Foundation for Innovation, the British Columbia Knowledge Development Fund, and Silicon Graphics at the University of Northern British Columbia.

References and Notes

(1) Boothroyd, A. I.; Martin, P. G.; Peterson, M. J. *J. Chem. Phys.* **2003**, *119*, 3187.
(2) Roberts, C. S. *Phys. Rev.* **1963**, *131*, 203.
(3) Karplus, M.; Kolker, H. J. *J. Chem. Phys.* **1964**, *41*, 3995.
(4) Kraus, M.; Mies, F. H. *J. Chem. Phys.* **1965**, *42*, 2703.
(5) Gordon, M. D.; Secrest, D. *J. Chem. Phys.* **1970**, *52*, 120.
(6) Gengenbach, R.; Hahn, C. *Chem. Phys. Lett.* **1972**, *15*, 604.
(7) Tsapline, B.; Kutzelnigg, W. *Chem. Phys. Lett.* **1973**, *23*, 173.
(8) Geurts, P. J. M.; Wormer, P. E. S.; van der Avoird, A. *Chem. Phys. Lett.* **1975**, *35*, 444.
(9) Wilson, C. W., Jr.; Kapral, R.; Burns, G. *Chem. Phys. Lett.* **1974**, *24*, 488.
(10) Tang, K. T.; Toennies, J. P. *J. Chem. Phys.* **1977**, *66*, 1496.
(11) Tang, K. T.; Toennies, J. P. *J. Chem. Phys.* **1978**, *68*, 5501.
(12) Dove, J. E.; Raynor, S. *Chem. Phys.* **1978**, *28*, 113.
(13) Russek, A.; Garcia, R. *Phys. Rev. A* **1982**, *26*, 1924.
(14) Schafer, J.; Köhler, W. E. *Physica* **1985**, *129A*, 469.
(15) Thakkar, A. J.; Hu, Z.-M.; Chauqui, C. E.; Carley, J. S.; LeRoy, R. J. *Theor. Chim. Acta* **1992**, *82*, 57.
(16) Muchnick, P.; Russek, A. *J. Chem. Phys.* **1994**, *100*, 4335.
(17) Truhlar, D. G.; Horowitz, C. J. *J. Chem. Phys.* **1978**, *68*, 2466; *J. Chem. Phys.* **1979**, *79*, 1514 (errata).
(18) Varandas, A. J. C.; Brown, F. B.; Mead, C. A.; Truhlar, D. G.; Blais, N. C. *J. Chem. Phys.* **1987**, *86*, 6258.
(19) Boothroyd, A. I.; Keogh, W. J.; Martin, P. G.; Peterson, M. J. *J. Chem. Phys.* **1991**, *95*, 4331.
(20) Boothroyd, A. I.; Keogh, W. J.; Martin, P. G.; Peterson, M. J. *J. Chem. Phys.* **1996**, *104*, 7139.
(21) Wu, Y.-S.; Kuppermann, A.; Anderson, J. B. *Phys. Chem. Chem. Phys.* **1999**, *1*, 929.
(22) Keogh, W. J. Ph.D. Thesis, University of Toronto 1992.
(23) Aguado, A.; Suarez, C.; Paniagua, M. *J. Chem. Phys.* **1994**, *101*, 4004.
(24) Boothroyd, A. I.; Martin, P. G.; Keogh, W. J.; Peterson, M. J. *J. Chem. Phys.* **2002**, *116*, 666.
(25) Boothroyd, A. I.; Martin, P. G.; Keogh, W. J.; Peterson, M. J. EPAPS Document No. E-JCPSA6-115-304140, 2002.
(26) McCourt, F. R. W.; Weir, D.; Clark, G. R.; Thachuk, M. *Mol. Phys.* **2005**, *103*, 17.
(27) Kalinin, A.; Komilov, O.; Rusin, L. Y.; Toennies, J. P. *J. Chem. Phys.* **2004**, *121*, 625.
(28) Gianturco, F. A.; Gonzalez-Lezana, T.; Delgado-Barrio, G.; Villarreal, P. *J. Chem. Phys.* **2005**, *122*, 084308.
(29) Lee, T.-G.; Rochow, C.; Martin, R.; Clark, T. K.; Forrey, R. C.; Balakrishnan, N.; Stancil, P. C.; Schultz, D. R.; Dalgarno, A.; Ferland, G. J. *J. Chem. Phys.* **2005**, *122*, 024307.
(30) Dove, J. E.; Rusk, A. C. M.; Cribb, P. H.; Martin, P. G. *Astrophys. J.* **1987**, *318*, 379.
(31) Draine, B. T.; McKee, C. F. *Annu. Rev. Astron. Astrophys.* **1993**, *31*, 373.
(32) Mandy, M. E.; M. Sc. Thesis, University of Toronto, 1980.
(33) Mandy, M. E.; Dove, J. E. *Astrophys. J.* **1986**, *311*, L93.
(34) Mandy, M. E.; Dove, J. E. *Int. J. Chem. Kinet.* **1986**, *18*, 993.
(35) Dove, J. E.; Raynor, S.; Teitelbaum, H. *Chem. Phys.* **1980**, *50*, 175.
(36) Gear, C. W. *Numerical Initial Value Problems in Ordinary Differential Equations*; Prentice Hall: Englewood Cliffs, NJ, 1971.
(37) Mandy, M. E.; Martin, P. G. *J. Phys. Chem.* **1991**, *95*, 8726.
(38) Mandy, M. E.; Martin, P. G. *J. Chem. Phys.* **1992**, *97*, 265.
(39) Kendall, M. G.; Stuart, A. *The Advanced Theory of Statistics*, 4th ed.; C. Griffin: London, 1979; Vol. 2.
(40) Mandy, M. E.; Martin, P. G.; Keogh, W. J. *J. Chem. Phys.* **1994**, *100*, 2671.
(41) Mandy, M. E.; McNamara, G. J. Manuscript in preparation.